Mon. Not. R. Astron. Soc. **343,** 775–780 (2003)

Determining the initial radius of meteor trains: fragmentation

M. Campbell-Brown★ and J. Jones
University of Western Ontario, London, Ontario N6A 3K7, Canada

Accepted 2003 April 14. Received 2003 February 27; in original form 2002 November 7

ABSTRACT

The initial radius of meteor ionization has significant effects on measured height distributions, velocity distributions and flux measurements of underdense echoes determined from meteor radar observations. Multifrequency radar observations are used to examine the effects of initial train radius. A model has been constructed to explain the observed distribution, and has been tested on the 2001 Geminids. It is shown that fragmentation accounts for the most significant part of the attenuation due to finite train size.

Key words: meteors, meteoroids.

1 INTRODUCTION

Knowledge of the initial radius of meteor trains and its variation with altitude is crucial for the determination of the fluxes and the orbital distribution of meteoroids because the initial train radius is one of the most important factors determining the attenuation of radar meteor echoes at a given wavelength.

Radar observations in the VHF range are convenient for studying meteors and hence meteoroids since they can be made at any time of the day, in any kind of weather, and can record echoes from large numbers of meteors automatically. While a continuously running meteor patrol radar can produce accurate rates of meteor echoes, the fluxes can only be determined accurately if all observing biases are accounted for. While the limiting magnitude and collecting area for a given source are straightforward to calculate and contribute little error to the fluxes, it is difficult to estimate the correction that must be applied to the raw fluxes for the destructive interference resulting from the non-zero initial radius.

When a meteoroid encounters the atmosphere, it produces a train of ionization several kilometres long. A typical meteor radar detects specular reflections from these trains, most of which are underdense because the train is radiatively thin and radiation is scattered from the entire cross-section of the train. Overdense echoes, which are caused by larger meteors, reflect radiation mainly from the surface of the cylinder of ionization and do not suffer from initial-radius effects.

For infinitely thin trains there would be no height-dependent attenuation, but, immediately on formation, the train begins to expand and quickly attains an initial radius much larger than the meteoroid in the interval that the ablated ions are thermalized. Echoes from trains of radius comparable with the radar wavelength are significantly attenuated as a result of the lack of phase coherence from the signals reflected from the different parts of the train cross-section. Since the atmosphere is less dense at larger heights, the initial radius will be larger and the attenuation greater. This effect is observed in all radar observations: the height distribution of echoes depends on the wavelength of observation. There is a 'height ceiling' for any frequency; no underdense echoes can be detected above this height due to the large size of the meteor trains.

Previous studies of initial radius have produced widely varying results. Simple models of the ionization trains produced by non-fragmenting meteoroids (e.g. Manning 1958) indicate that the initial radius should vary as the atmospheric mean free path, but studies using observations of echoes at multiple frequencies (Greenhow & Hall 1960; Baggaley 1970) show a much slower dependence. Hawkes & Jones (1975) suggested that fragmentation of rotating meteoroids could account for the discrepancy and showed that this would require neither unacceptable rotation rates nor unreasonable physical properties for the meteoroids. More recently, Jones (1995) pointed out that all the experimental studies until now have been based on the dubious assumption that the electron density within the train varies with radius in a Gaussian fashion. Jones was able to show that even the simplest collisional model of the formation of the train results in a markedly non-Gaussian radial electron-density profile that would go some way towards explaining the observed scatter in the calculated values of the initial radius. The shape of the electron-density profile determines the frequency dependence of the reflection coefficient. A Fourier–Bessel transform of the electron-density profile provides the frequency dependence. If the electron distribution in the train is Gaussian, the amplitude of an echo after attenuation will go as $\exp[4\pi(r_0/\lambda)^2]$, where r_0 is the initial radius of the train and λ is the wavelength of the radar. If the distribution is exponential (as found with the model of Jones 1995), the frequency dependence can easily be found by numerically performing the Fourier–Bessel transform and fitting a rational polynomial to the result. Both density profiles, Gaussian and exponential, were simulated in this work.

We have tried to incorporate into a new model all the likely factors that might affect the attenuation of meteor echoes and to assess the importance of each of them by fitting this theoretical model to multi-frequency radar meteor observations. In our initial study we have

★E-mail: mcampbel@rssd.esa.int

used observations made of the 2001 Geminids at three wavelengths. By using meteors belonging to one shower we eliminate effects of velocity and differing physical structure, providing the simplest possible case for determining initial radius. If the Geminid data can be successfully modelled, the study can be extended to sporadic meteors.

2 EQUIPMENT AND OBSERVATIONS

A three-frequency meteor radar system was designed to investigate the initial-radius problem. The system consists of three radars, identical except for frequency, which are co-located in Tavistock, Ontario, Canada (43°.264 N, 80°.772 W) and operate at 17.45, 29.85 and 38.15 MHz. Each system has a single transmitter and seven receivers, arranged in an interferometer that allows the altitude and azimuth of an echo to be measured to about a degree. The meteor heights can then be determined from the measured range. The transmit antennas are three-element yagis, 0.1 wavelengths from the ground, and all the receiver antennas are two-element yagis, 0.125 wavelengths above the ground. All antennas have a very broad beam that can detect meteors over most of the sky. The shape of the gain patterns of each antenna are nearly identical on all three systems: the small differences between them are included in the model to rule out any influence of this factor on the results. The systems have approximate limiting radar magnitudes around $+8^M$, depending on the transmitter powers, where the radar magnitude is a logarithmic function of the electron line density (McKinley 1961). The powers are monitored continuously on each system throughout the experiment; the peak powers on all systems vary between 5 and 6 kW for this period. The receiver calibrations on each system are also measured carefully during the experiment to account for any differences between the systems due to this factor, since the cable lengths from each antenna are different.

Meteor echoes are detected and recorded automatically on each system (for details, see Hocking, Fuller & Vandepeer 2001). The detection procedures discriminate against overdense echoes, leaving only the desired underdense echoes. Since overdense echoes are not affected by attenuation due to initial radius, the few overdense echoes that are recorded are removed in subsequent analysis.

During the 2001 Geminids, the 17-MHz system suffered severe terrestrial interference, resulting in low numbers of Geminid echoes. For this reason, only 29- and 38-MHz data were used in constructing the model, and 17-MHz data were used only to test the model.

Shower meteors were isolated by accepting only echoes occurring close to 90° from the Geminid radiant. This procedure inevitably allowed a few sporadic meteors into the data set, but because of the large number of Geminids recorded, the fraction of other meteors was estimated at less than 5 per cent. Echoes occurring within 20° of the horizon were rejected, since the height measurements are most uncertain at large ranges.

Some care was needed with the measurement of the echo amplitudes since there was no guarantee that the echo signal would be sampled at the instant that it reached its maximum amplitude. Ideally, each pulse sent by the transmitter would be square, with constant amplitude from beginning to end, and would need to be sampled only once. Since the pulses occupy a finite bandwidth of 50 kHz, the pulses are not perfectly rectangular and have tapered ends. If one radar happened to sample the pulse slightly off the maximum while the other sampled directly at the maximum, the amplitudes on each system would differ (Fig. 1).

For this reason, the pulse length was increased to 10 km (33.3 μs), and the sampling rate was raised so that each pulse was sampled

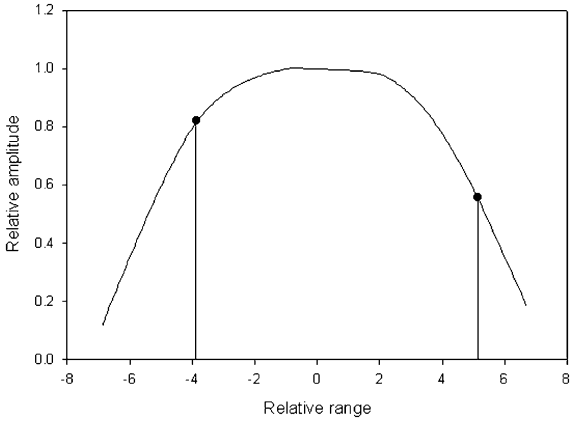

Figure 1. Example of a transmitted pulse with insufficient sampling.

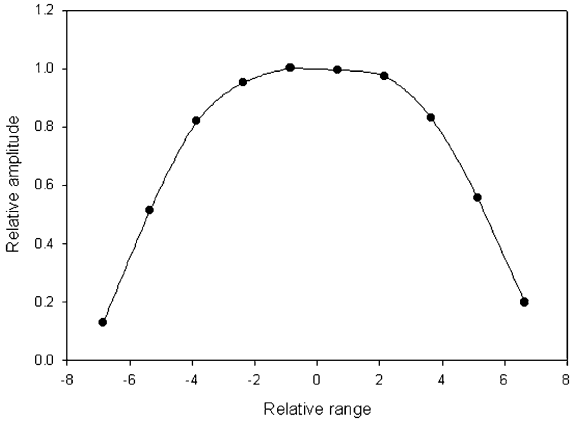

Figure 2. Actual 10-km pulse, sampled at 1.5-km intervals, on the 29-MHz system.

multiple times. The shape of returned radar pulses was carefully measured by sampling the pulse every 1.5 km (Fig. 2). We simulated echoes from meteors with various pulse lengths and sampling intervals to determine the minimum number of samples per pulse required to obtain an accurate estimate of the amplitude. Noise was added to each return in a random way. We found that, using a shaped pulse of width T, having a sampling interval between $0.3T$ and $0.4T$ was sufficient to find the maximum amplitude to within the noise limits. This could be sampling every 1.5 km for a 4 km pulse or every 3 km for a 8 km pulse. Not all meteors will be sampled the required three times, but because the tapered edges of the pulse extend past the width, most meteors with significant signal-to-noise ratios will.

The sampling rate was set to 3 km for 8 km pulses, and only those echoes that were sampled three times were accepted in the analysis. The three samples were then used to fit the known pulse shape and hence provided an accurate estimate of the maximum amplitude of the echo. This procedure ensured that faint meteors close to noise were excluded from the analysis. The best range was also determined from this procedure: errors in the range were of order 1.5 km. Together with the uncertainty in elevation angles as determined with the interferometer, this produces errors in the heights between 1.5 and 4 km, depending on the elevation of the echo. Once Geminid echoes with accurate height and amplitude information had been extracted, simultaneous echoes at 29 and 38 MHz were identified. The ratio of the amplitudes measured on each system was then plotted against the height of the meteor. Because of the geometry,

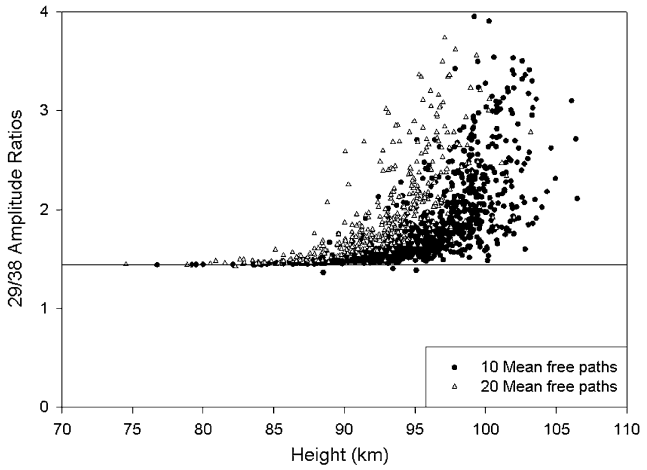

Figure 3. Expected distribution of amplitude ratios for simple initial train radius.

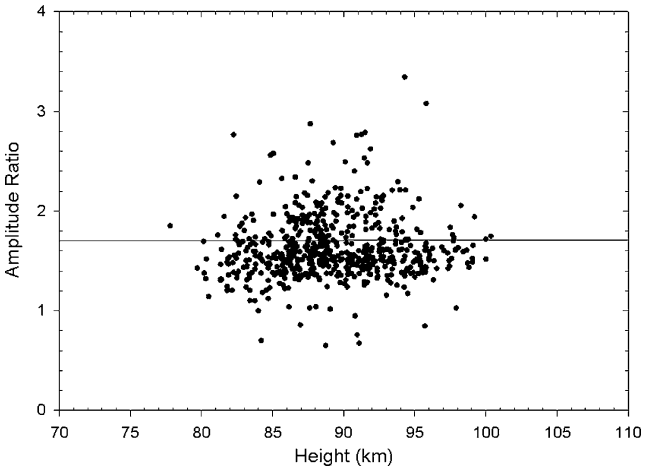

Figure 4. Amplitude ratios of 2001 Geminid meteors.

Geminid echoes occurred mainly between 08 and 15 UT (03 and 10 local time), and again between 23 and 05 UT (19 and 00 local time). Between 15 and 23 UT, the radiant is below the horizon, and between 05 and 08 UT, the echo line is below 20 degrees.

For single-body ablation we would expect the amplitude ratios to be constant with height at lower heights and to increase with height with a scatter reflecting the errors in the height and amplitude measurements as shown in Fig. 3, which depicts the results of a simple model based on the theory of Jones (1995). These include likely measurement errors, including height measurements, differences in the gain patterns of the antennas, and estimation of the maximum amplitude of the echoes. The horizontal line marks the limiting value of 1.44, which is the expected ratio of the 29- and 38-MHz amplitudes in the absence of initial-radius effects. Observations of four days of Geminid meteor data shown in Fig. 4 are in marked contrast to the predictions of the simple model with the observations showing much greater scatter than can be accounted for by the measurement errors in height and amplitude. Again, the horizontal line shows the expected ratio in the absence of initial-radius effects, here displaced from 1.44 because of differences in power between the two systems.

3 MODELLING DATA

The discrepancy between the observations and model predictions indicates that the additional scatter is the result of a frequency-dependent mechanism that could be the finite-velocity effect, Faraday rotation or fragmentation. The finite-velocity effect refers to the attenuation of the echo in the interval the meteoroid takes to cross the first Fresnel zone. According to Peregudov (1958) the finite-velocity attenuation is given by

$$\alpha = \frac{[1 - \exp(-\Delta)]}{\Delta} \tag{1}$$

where

$$\Delta = \frac{2k^2 D(2R_0\lambda)^{1/2}}{V}. \tag{2}$$

Although this expression assumes a radial Gaussian electron-density profile, which may not be correct, the attenuation was found to be small in practice and further corrections were deemed unnecessary.

Faraday rotation in the E- and F-regions of the ionosphere is another factor that is frequency dependent and so may contribute to scatter in amplitude ratios. In the case of the Geminids, which occur mainly during darkness when the ionosphere has a minimum electron density, Faraday rotation is not expected to have any significant effect. Nevertheless, the effect was included in the model in anticipation of modelling of sporadic meteors.

The finite-velocity and Faraday rotation effects were incorporated into our model of initial train radius. The train was modelled with a width of 10, 15 or 20 mean free paths and had a radial density with either a Gaussian or exponential cross-section. These values were chosen since they are consistent with simple collisional models of Manning (1958) and Jones (1995). In spite of these additional sources of frequency-dependent scatter, the agreement between model predictions and observations was only marginally improved and far from satisfactory.

At this point we were forced to consider that the source of the additional scatter might be fragmentation. Because we know from the success of methods used for the determination of shower radiants that the reflection process is highly specular, we conclude that the ionization trains are very smooth on the scale of the length of the first Fresnel zone. It is therefore unlikely that longitudinal irregularities along the train are the source of the scatter. We are left with transverse irregularities such as may be produced by a number of 'trainlets' separated by distances comparable with the radar wavelength.

The problem is how to deal with these trainlets quantitatively. There is much evidence from the smoothness of faint meteor light curves (Campbell et al. 2000) that meteoroids fragment before the onset of ablation and we have not attempted to model any continuous fragmentation. There are many parameters describing the fragmentation process: the size distribution and number of the particles, the radial distance of the particles from the meteor axis and its dependence on height, and the radial density distribution of particles. We will assume that the mass distribution of the fragments is well described by a power law:

$$\mathrm{d}n \sim m^{-s_\mathrm{f}}\,\mathrm{d}m. \tag{3}$$

As a starting point, the mass distribution index s_f of fragments from faint video meteor fragments was calculated using observations of sporadic meteors during the 2000 Leonid campaign. The light curves of the meteors were modelled with many values of s_f. Values between 1.6 and 2.0 were found to be consistent with the observations. The number of particles could not exceed 2000 for most small meteors, since including more fragments produces many fragments

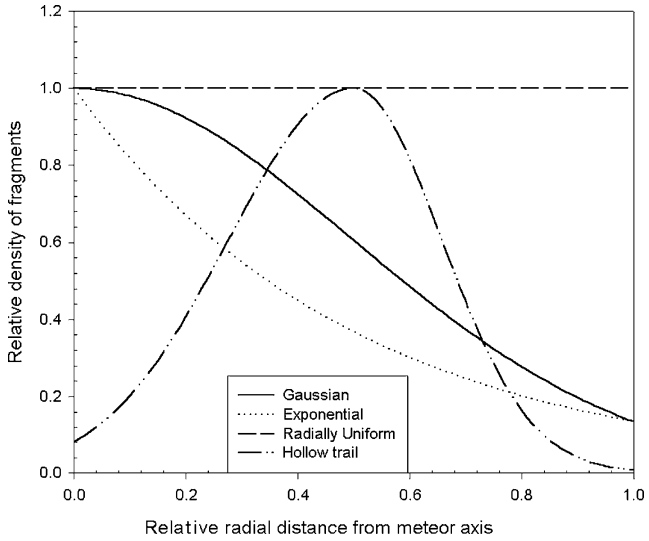

Figure 5. Possible radial density functions of fragments.

Table 1. Coefficients used in the simulation.

Shape of $n_e(r)$	Exponential	Gaussian		
$r_0(h) = n$ (mfp)	10	15	20	
Shape of $n_f(r)$	Radially constant	Gaussian	Hollow	$\exp(-\lvert x\rvert^5)$
s_f value of fragments	1.6	1.8	2.0	
Number of fragments	500	1000	2000	

too small to produce any luminosity or ionization; they reradiate more energy than they accumulate from collisions with atmospheric molecules and therefore do not ablate. The radius of fragmentation, or average distance of the particles from the meteoroid axis, was taken to vary linearly with height. Nothing is known about the radial distribution of the fragments, so several function were simulated: Gaussian, exponential, radially constant, hollow and a higher order exponential, $\exp(x^5)$ (Fig. 5).

In our model, there were six variable parameters in all:

(i) the shape of the electron-density function $n_e(r)$;
(ii) the height dependence of the initial radius (number of mean free paths);
(iii) the shape of the radial density of the fragments $n_f(r)$;
(iv) the height dependence of the radius of fragmentation: it is assumed that $r_f = Ah + B$;
(v) the s_f value of fragments: range from video observations;
(vi) the number of fragments.

Every combination of these parameters was simulated (Table 1), and a measure of goodness of fit obtained by comparing the simulation results with the observed data. Because of the large and significant scatter, the data were binned in both height and amplitude ratio and the number of echoes falling in each bin compared in the theoretical and observed cases. The cumulative error was the sum of the squares of the difference in each bin.

The results (shown in Table 2) show that the model is not very dependent on the number of particles, the radial distribution of the fragments, or the number of mean free paths in the initial radius of individual fragments. The s_f value of the fragments was found to be 1.8, and an exponential distribution of electrons in individual trains

Table 2. Best fits. In all cases listed the best-fitting radial electron-density distribution was exponential and the radius of fragmentation varied with height as $-0.01h + 2.4^a$[m].

Model	$n_f(r)$ shape	$r_e(h) = n$ (mfp)	s value	N_f	residual
001312	constant	10	1.8	2000	1.813
201312	Gaussian	15	1.8	2000	1.819
321310	hollow	20	1.8	500	1.822
201310	Gaussian	15	1.8	500	1.90
101311	high order	15	1.8	1000	1.93
221301	Gaussian	20	1.6	1000	2.10

Note. [a] h in km.

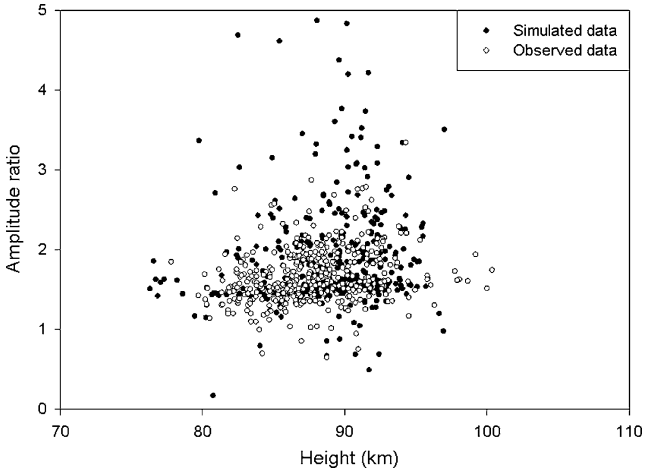

Figure 6. Observed and simulated Geminid amplitude ratios: 29/38 MHz.

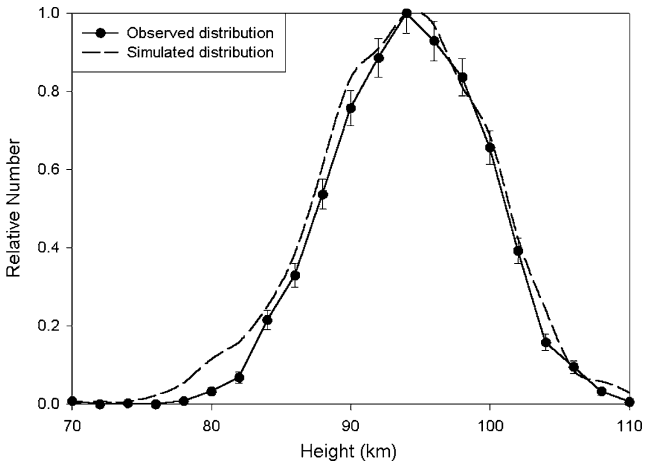

Figure 7. Observed and simulated Geminid height distributions: 17 MHz.

provided the best fit. The radius of fragmentation fitted best when decreasing with increasing height.

The model produced a good fit to the amplitude ratios of the 29- and 38-MHz systems (Fig. 6), but further tests are needed to have confidence in the model. The height distributions produced by the model at 29 and 38 MHz were therefore also compared, along with the 17-MHz height distribution. All three matched the observations very well (Figs 7, 8 and 9).

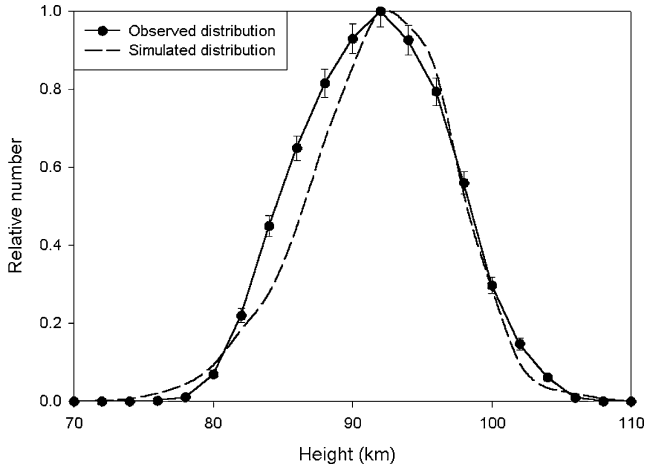

Figure 8. Observed and simulated Geminid height distributions: 29 MHz.

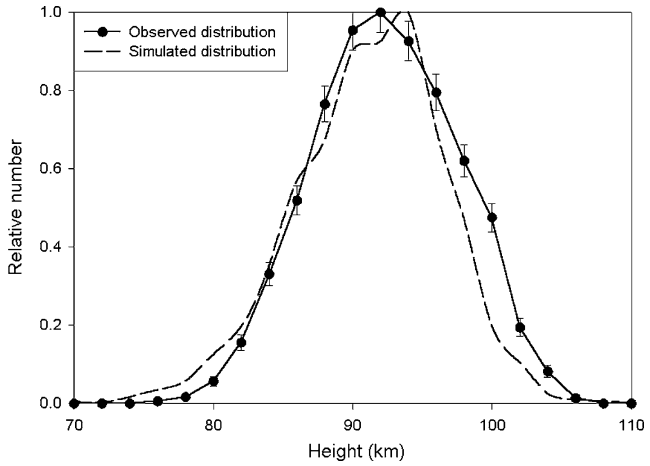

Figure 9. Observed and simulated Geminid height distributions: 38 MHz.

4 CORRECTION FACTOR

The fraction of meteors not detected because of initial-radius effects depends on the height distribution of the meteors being observed, and on the wavelength of observation. The height distribution of Geminids has been measured with optical techniques (Jacchia, Verniani & Briggs 1965; Hawkes & Jones 1980) as a function of limiting magnitude. The height at which the maximum number of meteors occur ($h_{\max}$) is related to the limiting magnitude, LM, by

$$h_{\max} = 95.6 - 1.77(\mathrm{LM} - 9) \tag{4}$$

By simulating data collected at a range of wavelengths and limiting magnitudes, a general correction factor can be calculated. The best fit was found to be

$$C_{\mathrm{Gem}}(h_{\max}, \lambda) = \left[1 + \exp\left(\frac{h_{\max}}{8.59} - \frac{\ln\lambda}{0.563} - 6.90\right)\right]^{-1}, \tag{5}$$

where C is the fraction of meteors that can be detected by a radar with the given limiting magnitude LM and wavelength λ in metres.

We must emphasize that the expression given above strictly applies only to Geminid meteor echoes and we do not know as yet how well it might apply to other meteors, even of the same speed and height of ablation.

5 FRAGMENTATION

One particularly interesting result of the model is the dependence of the radius of fragmentation on height. A decrease of initial radius with increasing height implies that fragments move away from the train axis after the meteoroid breaks up so that the transverse spread in fragments increases as they penetrate deeper into the atmosphere. Evidence from light curves (e.g. Campbell et al. 2000) implies that most small meteoroids fragment before the onset of luminous ablation, and therefore before the onset of ionization. Hawkes & Jones (1975) suggested that such a radial spreading of the fragments could be the result of rotation acquired from collisions in interplanetary space.

The radial speed, v_{r}, of the particles and the height at which they separate can easily be calculated from the radius of fragmentation found above. The radius of fragmentation, r_{f}, will be zero at 240-km altitude.

$$v_{\mathrm{r}} = -Av\cos z[\mathrm{m\,s^{-1}}], \tag{6}$$

where z is the zenith angle of the meteor radiant and A the slope of the radius of fragmentation function. The negative sign compensates for the fact that A is negative. Taking the zenith angle to be 45 °, we find the radial velocity of the Geminid fragments is 0.24 m s^{-1}.

If we assume that the radial spread of the meteoroid fragments is due to rotation of the meteoroid, we can calculate the angular frequency. If the particle is a sphere, the angular frequency can be found:

$$\omega = \frac{v_{\mathrm{r}}}{R} = v_{\mathrm{r}}\left(\frac{3m}{4\pi\rho}\right)^{-1/3}, \tag{7}$$

where R is the meteoroid radius, m its mass and ρ its density. The radial speed of the particle away from the axis of the train is its tangential speed immediately before it separates from the parent meteoroid. This assumes that the axis of rotation of the meteoroid is parallel to its trajectory in the atmosphere: if it is not, the meteor train formed by the fragments will have an ellipsoidal cross-section. To find the angular frequency of the rotating meteoroid from the radial velocity, one needs to make assumptions about the mass, density and shape of the meteoroid, none of which are well known for cometary meteoroids.

There is an upper limit on the angular frequency of a meteoroid past which the cohesive strength of the meteoroid material is insufficient to hold it together. Öpik (1958) derived the formula for rotational bursting, based on the size of the meteoroid and its tensile strength:

$$\omega_{\max} = \frac{1}{R}\left(\frac{S_{\mathrm{t}}}{\rho}\right)^{1/2} \tag{8}$$

where S_{t} is the tensile strength. If the meteoroid spins faster than this limit, the outer layers will break off. The tensile strength of meteoroids is very uncertain: for a stony meteoroid the tensile strength might be 2×10^8 N m^{-2}; for a fragile cometary meteoroid the value would be much lower, of order 2×10^3 N m^{-2} (Whipple 1963). A cometary meteoroid of mass 10^{-5} kg could not spin faster than 10^3 rad s^{-1}; a meteoroid at the radar's detection limit of about 10^{-9} kg would have to spin slower than 10^4 rad s^{-1}.

For the Geminids, the best estimate of the height of fragmentation was 240 km; heights between 220 and 260 km produced results within 5 per cent of this value. Assuming a density of 1500 kg m^{-3} and an average mass of 10^{-9} kg, the angular frequency of the Geminid meteors is 4500 rad s^{-1}, with an estimated error of 500 rad s^{-1}, which is quite consistent with the value of 10^4 rad s^{-1} predicted if the rotation rates are limited by rotational bursting.

6 CONCLUSIONS

The work presented here attempts to bring order into the confusion surrounding the initial radius of meteor trains and its variation with height. By including the effects of fragmentation, we have built on the work of Jones (1995), who questioned the long-standing unsubstantiated assumption of a Gaussian radial electron-density distribution. We have fitted a comprehensive model to radar observations of the Geminid shower made at 29 and 38 MHz, and determined a set of parameters that gives a good description of simultaneous independent data acquired at 17 MHz on an otherwise identical radar. So far as we are aware, this is the first time that such a study has been possible.

While the uncertainties are large, the radial spread of the meteoroid fragments is of particular interest. The fragmentation model that best fits the data is consistent with the rotating meteoroid model proposed by Hawkes & Jones (1975). Further observations, particularly at lower frequencies where greater heights can be sampled, may reduce the errors and allow a more accurate estimate of the height at which fragmentation occurs – which would help identify the process by which meteoroids fragment and would have implications for the chemical composition of the meteoroids. If fragmentation does occur at very large altitudes, a new mechanism would have to be found to account for it, since it is well above the classical heating regime.

We have obtained a formula for correcting the apparent fluxes of Geminid meteors at a given height. Clearly, this is of limited value – but we intend to expand this study to include other showers as well as sporadic meteors. In particular we intend to investigate the effects of meteor speed on the initial train radius.

ACKNOWLEDGMENTS

Funding from the Natural Sciences and Engineering Research Council of Canada and NASA is gratefully acknowledged. The authors would also like to thank the reviewer for many helpful comments.

REFERENCES

Baggaley W. J., 1970, MNRAS, 147, 231
Baggaley W. J., 1980, Bull. Astron. Inst. Czechosl., 31, 308
Baggaley W. J., 1981, Bull. Astron. Inst. Czechosl., 32, 345
Baggaley W. J., Fisher G. W., 1980, Planet. Space Sci., 28, 575
Bayrachenko I. V., 1963, Geomag. & Aer., 5, 353
Bronshten V. A., 1983, The Physics of Meteoritic Phenomena. Reidel, Dordrecht
Campbell M. D., Hawkes R. L., Babcock D. D., 1999, Proc. Int. Conf. Meteoroids 1998. Slovak Acad. Sci., Bratislava, p. 363
Campbell M. D., Brown P. G., LeBlanc A. G., Hawkes R. L., Jones J., Worden S. P., Correl R. R., 2000, Meteorit. & Planetary Sci., 35, 1259
Greenhow J. S., Hall J. E., 1960, MNRAS, 121, 183
Hawkes R. L., Jones J., 1975, MNRAS, 173, 339
Hawkes R. L., Jones J., 1978, MNRAS, 185, 727
Hawkes R.L., Jones, R.L., 1980, in Halliday I., McIntosh B. A., eds, Solid Particles in the Solar System, p. 117
Hocking W. K., Fuller B., Vandepeer B., 2001, J. Atmospheric Sol. Terrest. Phys., 63, 155
Jacchia L. G., Verniani F., Briggs R. E., 1965, Smithsonian Astrophysical Observatory Special Report, 175
Jones W., 1995, MNRAS, 275, 812
Manning L. A., 1958, J. Geophys. Res., 63, 181
McKinley D. W. R., 1961, Meteor Science and Engineering. McGraw-Hill, New York
Murray I. S., Beech M., Taylor M. J., Jenniskens P., Hawkes R. L., 2000, Earth, Moon and Planets, 82, 351
Öpik E. J., 1958, Physics of Meteor Flight in the Atmosphere. Interscience Publishers, New York
Peregudov F. I., 1958, Sov. Astron., 2, 833
Whipple F. L., 1963, Smithsonian Centr. Astrophys., 7, 239

This paper has been typeset from a TEX/LATEX file prepared by the author.